Optics & Laser Technology 76 (2016) 106–112

Contents lists available at ScienceDirect

Optics & Laser Technology

journal homepage: www.elsevier.com/locate/optlastec

Effect of different EBL structures on deep violet InGaN laser diodes performance

Gh. Alahyarizadeh [a,*], M. Amirhoseiny [a,b], Z. Hassan [c]

[a] Engineering Department, Shahid Beheshti University, G.C., P.O. Box 1983969411, Tehran, Iran
[b] Department of Engineering Science, Buein Zahra Technical University, Buein Zahra, Qazvin, Iran
[c] Nano-Optoelectronics Research and Technology Laboratory, School of Physics, University Science USM, Malaysia, 11800 Penang, Malaysia

ARTICLE INFO

Article history:
Received 10 March 2015
Received in revised form
1 August 2015
Accepted 5 August 2015

Keywords:
InGaN DQW laser diode
Quantum well
Electron blocking layer
Quaternary
Numerical simulation

ABSTRACT

Some specific designs on band structure near the active region, including the modifications of the material and thickness of the electron blocking layer (EBL), in the deep violet InGaN laser diodes (LDs) are investigated numerically with the ISE TCAD software. The analyses focus on electron and hole carrier injection efficiency, carrier distributions, electron leakage, and radiative recombination, subsequently, optical material gain, and optical intensity. The results indicate that for the ternary AlGaN EBL, the lowest threshold current and the highest output power, slope efficiency, and DQE have been obtained for the 15 nm EBL thickness with 0.22 Al mole fraction. In addition, a comparative study has been conducted on the performance characteristics of the LD structures with a ternary AlGaN EBL and a quaternary AlInGaN EBL with an output emission wavelength at 390 nm. The simulation results showed that the using quaternary AlInGaN EBL effectively improves the LD performance characteristics.

1. Introduction

Recently, III-Nitride materials have attracted significant interest because of their specific properties including wide bandgap energy, broad coverage of the electromagnetic spectrum, and high thermal stability, as well as their wide application especially in optoelectronics as light sources, including full color display, illumination, high-density data storage, laser printing, biological agent detection systems, and medical applications [1–5]. InGaN violet quantum well lasers have promised the next generation of laser sources which will have safe and wide applications for high density optical disc systems such as Blue ray Disc (BD) and HD-DVD, and other applications. Although these types of LDs are commercialized, superior performance and shorter output emission wavelength are anticipated as challenges for the next generation of laser sources [6–8]. Reducing the threshold current and improving stimulated efficiency are two of the approaches used to attain superior performance. Electron overflow from the active region into the p-side layers, such as p-GaN waveguide and p-AlGaN cladding layers, is the important occurrence which increases threshold current and decreases stimulated efficiency, and consequently the performance of InGaN multi quantum well (MQW) LDs. Inserting a thin AlGaN electron blocking layer (EBL) between the last barrier and p-waveguide layer is the first solution to overcome the electron overflow problem. The AlGaN EBL prevents electron overflow, and protects the InGaN active region from the high temperature growth of next p-type layers [9,10]. Various EBL designs, such as quaternary AlInGaN [11,12] multi-quantum-barrier (MQB) AlGaN/GaN [13,14] combined AlGaN bulk and MQB and step-graded EBLs [15–20] are available to control the electron overflow and improve the performance of InGaN LDs. Results from these designs indicate that the built-in polarization and related induced charge at the interface of the last barrier and EBL can be compensated using a quaternary AlInGaN EBL with appropriate Al and In compositions [6,17].

Moreover, although using AlGaN EBL improves InGaN LDs performance, the induced charge at the interface of the last barrier and the EBL resulting from polarization mismatch changes the valence band offset at the interface, thus obstructing the transport of holes. This situation leads to non-uniform distribution of electron and hole carriers in wells which, may induce light absorption at times and decrease LD performance. Still, studies support the view that EBL is essential to InGaN LDs [16,21]. This contradiction in using AlGaN EBL remains as a challenge for researchers dealing with III-nitride devices, especially LED. Another way to overcome the aforementioned problems is to use AlInGaN quaternary EBL to reduce non-uniform distributions [16,22].

In this paper, the effects of Al composition and thickness of AlGaN EBL on optical and electrical properties of deep violet $In_{0.082}Ga_{0.918}N$/GaN DQW LDs have been investigated. In addition,

* Corresponding author.
E-mail address: g_alahyarizadeh@yahoo.com (Gh. Alahyarizadeh).

http://dx.doi.org/10.1016/j.optlastec.2015.08.007
0030-3992/

a comparative study has been conducted on the performance characteristics of the LD structures with an AlGaN EBL and a quaternary AlInGaN EBL with an output emission wavelength at 390 nm.

2. Laser structure and simulation parameters

The schematic diagram of deep violet $In_{0.082}Ga_{0.918}N$/GaN DQW LD structures under study are shown in the Fig. 1. The original structure with AlGaN EBL which is a modified structure of the laser structure fabricated by Nakamura et al. consists of a 0.4 μm n-GaN layer, a 0.1 μm n-$In_{0.05}Ga_{0.95}N$ compliance layer, a 0.5 μm n-$Al_{0.07}Ga_{0.93}N$ cladding layer, a 0.1 μm n-GaN waveguide layer, a 2.5/8.5 nm $In_{0.082}Ga_{0.918}N$/GaN DQW active region, a 10–30 nm p-$Al_xGa_{1-x}N$ EBL, a 0.1 μm p-GaN waveguide layer, a 0.5 μm p-$Al_{0.07}Ga_{0.93}N$ cladding layer and a 0.1 μm p-GaN layer, respectively [23–25]. The doping concentrations of n- and p-type layers are 5.5×10^{18} and 1.3×10^{18} cm^{-3}, respectively. The laser area is 1 μm*300 μm, and the reflectivity of the back and front mirrors is equal to 50%.

The laser simulation was conducted by solving several sets of equations, including the Schrodinger, Poisson, photon-rate, current continuity, and scalar wave equations. The simulator also includes a carrier drift-diffusion model that contains Fermi statistics and incomplete ionization [6].

The physical parameters of the ternary and the quaternary alloys used in the simulation were interpolated by binary alloys that can be expressed by the following equation:

$$Q_{Al_xIn_yGa_{1-x-y}N} = x \cdot Q_{AlN} + y \cdot Q_{InN} + (1 - x - y) \cdot Q_{GaN}, \quad (1)$$

where Q_{InN}, Q_{GaN}, and Q_{AlN} are the physical parameters of InN, GaN, and AlN, such as effective masses, refractive index, and others as listed in Table 1 [6]. The above equation applies to all physical parameters except for band gap energy, which can be expressed by the following equations [6]:

$$E_g(\mathrm{AlInGaN}) = \frac{xyE_g^u(\mathrm{AlInN}) + yzE_g^v(\mathrm{InGaN}) + xzE_g^w(\mathrm{AlGaN})}{xy + yz + zx}, \quad (2)$$

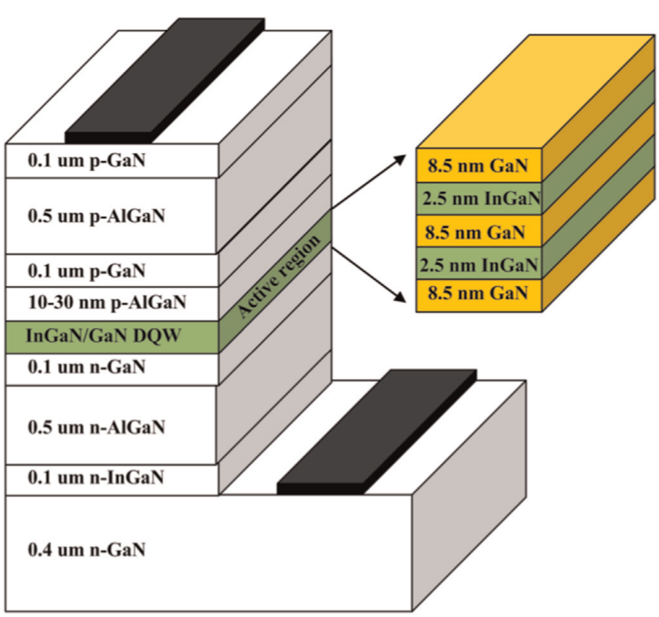

Fig. 1. Schematic diagram of laser structures of deep violet InGaN DQW LDs with AlGaN EBL.

Table 1
Room temperature properties of binary III-N materials [6].

Parameters	GaN	AlN	InN
Bandgap energy E_g (eV)	3.47	6.28	0.8
Electron affinity (eV)	4.1	1.9	5.8
Lattice constant a_0(°A)	3.189	3.112	3.545
Spontaneous polarization P_{sp}	−0.034	−0.09	−0.042
Refractive index near E_g	2.506	2.035	2.9
Electron effective mass	0.22 m_e	0.4 m_e	0.11m_e
Heavy hole effective mass	1.595 m_e	2.68 m_e	1.449 m_e
Light hole effective mass	0.261 m_e	0.261 m_e	0.157 m_e
Elastic stiffness constant C_{13}(GPa)	106	108	92
Elastic stiffness constant C_{33}(GPa)	398	373	224
Relative dielectric constant	8.9	8.5	9.5

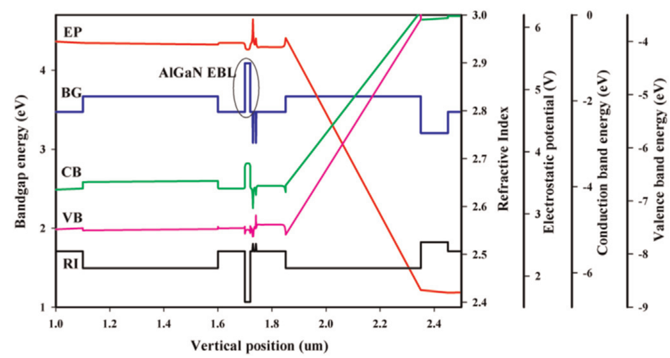

Fig. 2. Energy band diagrams (band gap, valence band and conduction band energy), electrostatic potential and refractive index of deep violet $In_{0.082}Ga_{0.918}N$/GaN DQW LD.

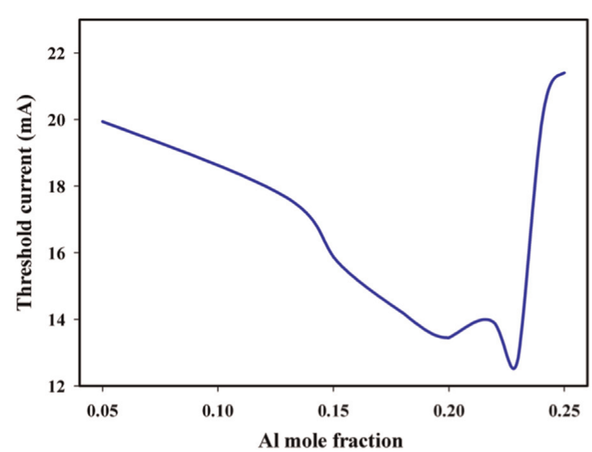

Fig. 3. Threshold current of $In_{0.082}Ga_{0.918}N$ DQW LD as a function of Al composition of EBL with 20 nm thickness.

$$E_g^u(\mathrm{AlInN}) = u \cdot E_g(\mathrm{InN}) + (1 - u) \cdot E_g(\mathrm{AlN}) - u \cdot (1 - u) b(\mathrm{AlInN}), \quad (3)$$

$$E_g^v(\mathrm{InGaN}) = v \cdot E_g(\mathrm{GaN}) + (1 - v) \cdot E_g(\mathrm{InN}) - v \cdot (1 - v) b(\mathrm{InGaN}), \quad (4)$$

$$E_g^w(\mathrm{AlGaN}) = w \cdot E_g(\mathrm{GaN}) + (1 - w) \cdot E_g(\mathrm{AlN}) - w \cdot (1 - w) b(\mathrm{AlGaN}), \quad (5)$$

$$u = \frac{1 - x + y}{2}, \quad v = \frac{1 - y + z}{2}, \quad w = \frac{1 - x + z}{2}, \quad (6)$$

where x, y, and $z = 1 - x - y$ are the compositions of aluminum, indium, and gallium in the AlInGaN, respectively. E_g(InN), E_g(GaN), and E_g(AlN) are the band gap energies of InN, GaN, and AlN,